

Modeling The Drying Of An Unsaturated Deformable Porous Medium: Application To Packaging Kraft Paper

Belgacem CHANDOUL^{1,2*} , Maryem Fezai² and Mouna Elakhdar²

¹Higher Institute of Technological Studies of Tataouine, Almahragène City - 1121 Tataouine - Tunisia

² Research Laboratory: Energy and Environment, National Engineering School of Tunis, 2092, Manar II, Tunis, Tunisia

*Corresponding Author

Belgacem CHANDOUL, Higher Institute of Technological Studies of Tataouine, Almahragène City - 1121 Tataouine – Tunisia.

Submitted: 2026, Mar 23; Accepted: 2026, Apr 20; Published: 2026, May 28

Citation: CHANDOUL, B., Fezai, M., Elakhdar, M. (2026). Modeling The Drying Of An Unsaturated Deformable Porous Medium: Application To Packaging Kraft Paper. *Adv Envi Wast Man Rec*, 9(1), 01-07.

Abstract

The main objective of this work is to model heat transfer in Kraft paper during drying. The model developed takes into account BIOT's assumptions regarding a uniform temperature environment; the paper used is assumed to be thermally thin (BIOT number $Bi < 0.1$). The results obtained are experimentally validated. They allowed us to show that the two drying phases of Kraft paper can be modeled by a thermal capacitor that charges upon contact with the drying cylinder (phase 1) and discharges into the free space (phase 2).

Keywords: Allium Roseum, Germination Characteristics, Seed Bank and Tunisia

1. Introduction

Kraft packaging paper is a porous, deformable, and unsaturated material composed of cellulose fibers [1]. Drying is an essential step in the manufacturing process, during which heat and mass transfer play a crucial role. This operation must be carefully controlled to preserve the paper's mechanical properties, which are highly sensitive to temperature and humidity variations [2,3].

Several recent studies have investigated heat and mass transfer in paper during drying [4,5]. The present work falls within this

theme. It is based on Biot's hypotheses applied to a thin medium, considering paper as a material at a uniform temperature ($Bi < 0.1$). Measurements carried out on an industrial machine allowed for the experimental validation of the proposed model. The two drying phases of Kraft paper are thus interpreted as the behavior of a thermal capacitor, which charges upon contact with the drying cylinder and discharges into the free space. Figure 1 shows the two drying phases of KRAFT paper in the PM2 machine dryer at SOTIPAPIER.

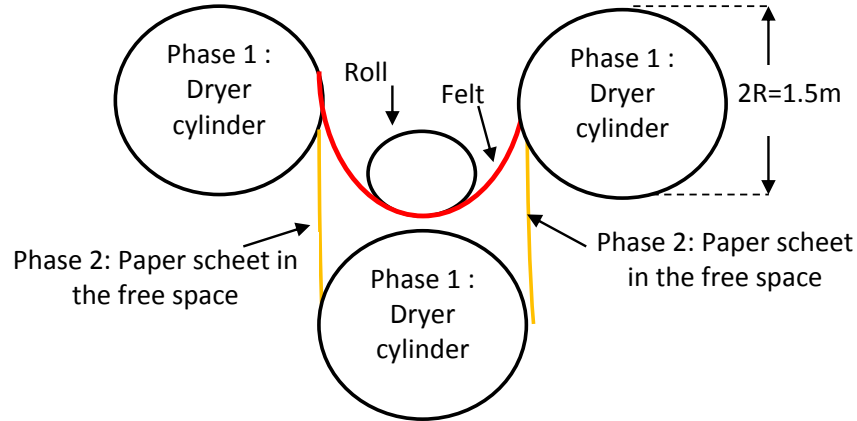


Figure 1: Drying Phases [6]

2. Theoretical study: Problem formulation

2.1 Hypotheses

In both drying phases, we assume:

- The surrounding environment is at a uniform temperature T_0 .
- The energy state of the paper at the beginning of the first phase is taken as the reference state.

- The paper is thermally thin: Uniform temperature environment (BIOT number < 0.1).
- The length L of the paper under study is equal to the length of the embracing arc.
- The width of the paper is $\ell = 3.16$ m.
- The embracing angle is $\alpha = 120^\circ$ (Figure 2).

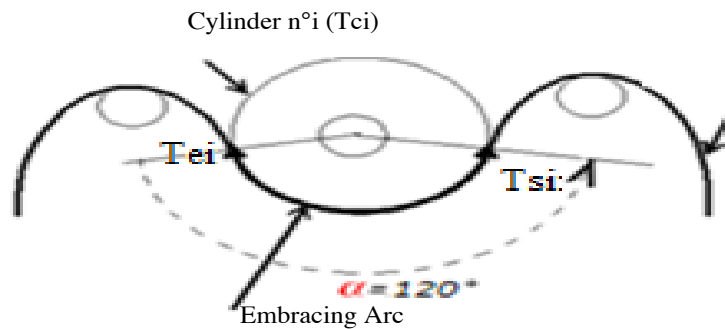


Figure 2: Embracing Arc

2.2 Thermal Balance Of The First Phase

The paper in contact with the drying cylinder $n^{\circ}i$, at temperature

T_{ci} , receives heat and its temperature increases. The heat balance is written as:

$$\begin{aligned}
 & \underbrace{\rho C_p V (T_{ci} - T_0)}_{\text{Maximum energy output of the drying cylinder}} \\
 & = \underbrace{\rho C_p V \frac{dT}{dt}}_{\text{Heat received by the paper sheet}} \\
 & + \underbrace{hs(T - T_0)}_{\text{Heat lost to the surrounding environment}} \quad (1)
 \end{aligned}$$

We pose : $\theta = T - T_0$ et $\tau = \frac{\rho C_p V}{hS}$; Equation (1) becomes:

$$\theta_{ci} = \frac{d\theta}{dt} + \frac{1}{\tau} \theta \quad (2)$$

The solution to equation (2) is of the form:

$$\theta(t) = A + B \cdot \exp\left(-\frac{1}{\tau} t\right) \quad (3)$$

Which gives, using boundary conditions ; $\theta(0)=0$ et $\theta(\infty)=\theta_c = T_c - T_0$:

$$\frac{T - T_0}{T_{ci} - T_0} = 1 - \exp\left[-\frac{1}{\tau} t\right] \quad (4)$$

2.3 Thermal Balance Of The Second Phase

In the free space between the upper ($n^{\circ}i$) and lower ($n^{\circ}i+1$) cylinders, the paper at temperature T_{si} releases heat to the

surrounding medium, at a uniform temperature T_0 , and its temperature decreases. The heat balance between t and $t+dt$ is written as:

$$\underbrace{-\rho C_p V \frac{dT}{dt}}_{\text{Heat released by the paper sheet}} = \underbrace{hs(T - T_0)}_{\text{Heat transferred to the surrounding environment}} \quad (5)$$

Either:

$$\frac{dT}{T - T_0} = -\frac{hs}{\rho C_p V} dt = -\frac{h}{\rho C_p e} dt \quad (6)$$

Which gives, by integration:

$$\frac{T - T_0}{T_{si} - T_0} = \exp\left[-\frac{h}{\rho C_p e} t\right] \quad (7)$$

2.4 Thermal Capacitor Model

Equations (4) and (7) show that the drying of Kraft paper can be interpreted as a thermal capacitor that charges during the first

phase and discharges during the second phase (Figure 3). The time constant is:

$$\tau = \left(\frac{1}{hS}\right) \cdot \underbrace{(\rho C_p V)}_{\text{Thermal capacity}}$$

The thermal capacitor model is shown in Figure 4

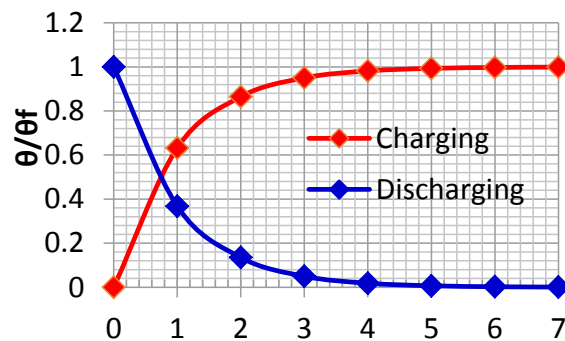


Figure 3: Charging and discharging of the thermal capacitor

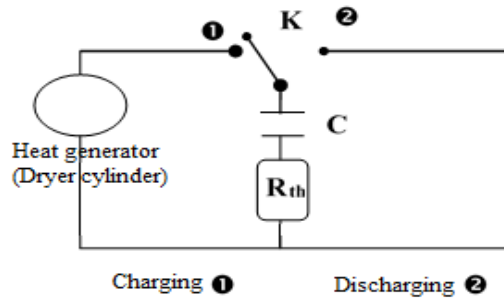


Figure 4: Thermal Capacitor Model

3 Experimental study

3.1 Material and Method

The experiment was conducted on kraft paper with a basis weight of 70 g/m² during drying. The experimental conditions were as follows:

- Machine speed: U1=260m.mn-1, U2=280m.mn-1, U3=310m.mn-1.
- The thickness of the sheet is assumed to be constant; e= 0.119

mm.

- The specific heat capacity of kraft paper is: Cpf = 1,34 kJ.kg-1.K-1.

- The kraft paper thermal conductivity is: λf = 1,34 W.m-1. °C-1. [7]

- The kraft paper density is: ρf = 1340 kg.m-3.

- Air characteristics at average temperature air-paper (30°C): Table 1

| Density ρ (kg.m-3) | Dynamic viscosity | Specific heat capacity C (J.kg-1.K-1) | Thermal conductivity λ (W.m-1.K-1) | Prandtl. number Pr |
|--------------------|-------------------|---------------------------------------|------------------------------------|--------------------|
| 1,177 | 1,85×10-5 | 1006 | 0,0262 | 0.708 |

Table 1: Air Characteristics at 30°C [8]

3.2 Measurements

The pressure is set at the press section of the SOTIPAPIER (TUNISIA) kraft paper manufacturing machine, and consequently, the moisture content x0, sch at the press outlet is set. The steam flow rate is then adjusted to ensure a fixed moisture content x1,

sch at the dryer outlet. Using appropriate probes, the temperature TC of the drying cylinders, as well as those of the sheet Te and TS respectively, before and after its contact with these cylinders are measured. The measurements are shown in Table 2.

| Cylinder n° | Tc | Te= T0 | Ts | Cylinder n° | Tc | Te= T0 | Ts |
|-------------|-------|--------|------|-------------|------|--------|------|
| 1 | 70 | 30,9 | 31,6 | 15 | 90,7 | 62,2 | 76,4 |
| 2 | 48,4 | 31,3 | 36,4 | 16 | 97,6 | 67 | 72,7 |
| 3 | 54,2 | 37,3 | 52,7 | 17 | 98,2 | 70,4 | 81,5 |
| 4 | 49,2 | 50 | 45,3 | 18 | 82,4 | 72,1 | 68,8 |
| 5 | 69 | 47,8 | 58,3 | 19 | 51,3 | 45,7 | 50,1 |
| 6 | 92,6 | 56,1 | 82,2 | 20 | 83,2 | 47,2 | 77,8 |
| 8 | 70,6 | 68,9 | 64,7 | 21 | 51,7 | 69,3 | 53,4 |
| 9 | 91 | 59,8 | 73,9 | 22 | 85 | 50,2 | 82,6 |
| 10 | 85,6 | 61,3 | 74,1 | 23 | 76,9 | 72,6 | 75 |
| 11 | 93,6 | 67,9 | 82,2 | 24 | 88,1 | 73,6 | 79,4 |
| 12 | 98,4 | 66,2 | 70,5 | 25 | 95 | 72,6 | 82,7 |
| 13 | 100,4 | 67,9 | 84,9 | 26 | 88,8 | 79,4 | 74,8 |
| 14 | 102,6 | 73,4 | 78,7 | | | | |

Table 2: Temperature Variation of The Drying Sheets and Cylinders

3.3. Determination of the Convection Coefficient h

The second phase can be interpreted as gas at temperature T_0 flowing at speed U over a large paper plate: length $L=R\alpha$, width l , and thickness e (Figure 5), in forced thermal convection. The dimensional analysis, aimed at determining the

convection coefficient h , involves determining the REYNOLDS

($Re = \frac{\rho U L_c}{\mu}$) and NUSSELT ($Nu = \frac{h L_c}{\lambda}$) numbers.

$L_c = \text{Volume/Section} = \frac{2 \cdot L \cdot l \cdot e}{l \cdot e} = 2L$: Characteristic length:

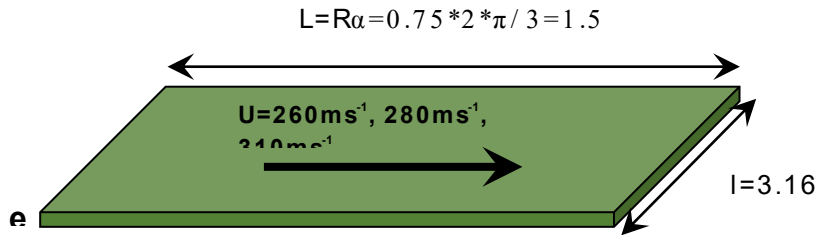


Figure 5: Equivalent System of the 2nd Drying Phase

- REYNOLDS number ($Re = \frac{\rho U L_c}{\mu}$)

Table 3 shows the REYNOLDS number values for the machine's three speeds.

| U(m/mn) | 260 | 280 | 310 |
|---------|----------|----------|----------|
| Re | 8,67.105 | 5,97.105 | 6,48.105 |

Table 3 : Reynolds Number Values

The regime is, therefore, turbulent given that $Re > Rec = 3.10^5$

- NUSSELT number ($Nu = \frac{h L_c}{\lambda}$) will be determined by the following formula since the regime is turbulent.

$$Nu = 0.029 \cdot Re^{4/5} \cdot Pr^{1/3} \quad (8)$$

Table 4 shows the NUSSELT number values for the machine's three speeds.

| U(m/mn) | 260 | 280 | 310 |
|---------|---------|---------|---------|
| Nu | 1454,88 | 1542,73 | 1673,51 |

Table 4: Reynolds Number Values

- The convection coefficient h can be easily determined by: ($h = \lambda Nu / L_c$).

Table 5 shows the convection coefficient h values for the machine's three speeds.

| U(m/mn) | 260 | 280 | 310 |
|----------|-------|-------|-------|
| h(W/m2K) | 12,14 | 12,87 | 13,96 |

Table 5: Convection Coefficient h

For each thermal capacitor (cylinder n° i followed by a free space), the uniform temperature $T_0 = T_e$ will be taken according to measurements taken on the machine.

The results obtained for the three machine speeds allowed us to plot the curves in Figures 6, 7, and 8:

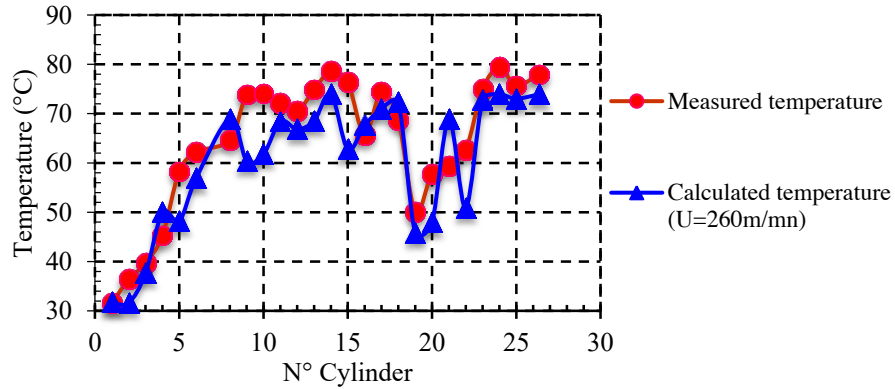


Figure 6: Measured and Calculated Temperatures TSI of the Paper at The Outlets of Cylinders $n^{\circ}i$ for $U= 260$ m/mn

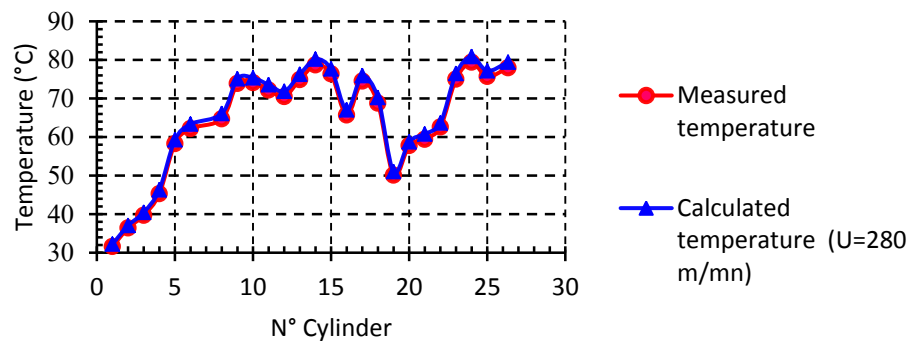


Figure 7: Measured and Calculated Temperatures TSI of the Paper at The Outlets of Cylinders $n^{\circ}i$ for $U= 280$ m/mn

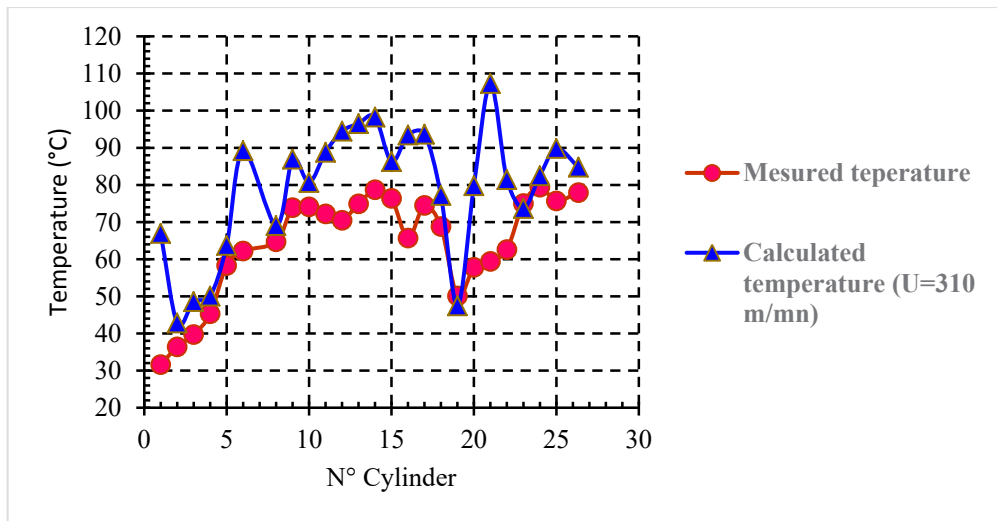


Figure 8: Measured and Calculated Temperatures TSI of the Paper at The Outlets of Cylinders $n^{\circ}i$ for $U= 310$ m/mn

The paper temperatures T_{si} at the outlet of each cylinder were determined from the equation of the first phase. The inlet temperatures T_{ei} can be obtained analogously using the equation of the second phase.

The curves obtained for the three speeds show good agreement between the experimental measurements and the values predicted

by the thermal capacitor model. The average relative error is less than 5%, which confirms the reliability of the proposed model.

In particular, we observe that the speed $U = 280$ m/min provides the best match, which can be explained by:

- Higher measurement accuracy,
- More stable aerodynamic conditions in free space,

- A better established forced convection regime.

4. Advanced Validation

The model-experiment comparison shows an average relative error of less than 5%, highlighting the model's relevance. The speed $U = 280$ m/min offers the best accuracy, likely due to a stabilized aerodynamic regime, which promotes homogeneous forced convection. A more detailed analysis also shows that the thermal dynamics are strongly influenced by the uniformity of the air-temperature gradient in this configuration.

5. Conclusion

In this work, we modeled heat transfer in Kraft paper during the drying process, representing the two phases with a thermal capacitor model. The paper is thermally charged in contact with the cylinders (phase 1) and discharged into the free space (phase 2).

The model is based on Biot's assumptions, which are valid for a thermally thin material. Comparisons between theoretical results and experimental measurements show very good agreement, thus validating the relevance of the proposed model.

The best results were obtained at a speed of 280 m/min, suggesting that the model is particularly well-suited to optimal forced convection conditions.

Acknowledgment

The authors express their sincere gratitude to Professor Lakder KAIROUANI and to the SOTIPAPIER company which supported this work.

Nomenclature

| | |
|----------|---|
| Bi | BIOT number |
| C_{pr} | Paper specific heat capacity (kJ.kg ⁻¹ . K ⁻¹) |
| e | Thickness paper sheet (m) |
| h | Convection coefficient (W/m ² K) |
| L_c | Characteristic length (m) |
| L | Embracing arc length (m) |
| ℓ | The sheet paper width (m) |
| Nu | NUSSELT number |
| Pr | Prandtl number |

| | |
|----------------|--|
| Re | REYNOLDS number |
| T0 | Temperature of the surrounding environment (°C) |
| Tci | Temperature of cylinder n ^o i (°C) |
| Tei | Paper sheet temperature at the cylinder inlet n ^o i (°C) |
| Tsi | Paper sheet temperature at the cylinder outlet n ^o i (°C) |
| U | Machine speed (m/s) |
| α | embracing angle (rad) |
| τ | Time constant (s) |
| λ _r | Paper thermal conductivity (W.m ⁻¹ .°C ⁻¹) |
| ρ _f | Paper density (kg.m ⁻³) |

References

1. Sahneu, N. L., & Back, E. L. (1985). Effects of temperature and moisture on the tensile properties of packaging papers. *Papper ja Puu*, 8, 477–481.
2. Uesaka, T. (1994). General formula for hygroexpansion of paper. *Journal of Materials Science*, 29, 2373–2377.
3. Niskanen, K. J., Kuskowski, S. J., & Bronkhorst, C. A. (1997). Dynamic hygroexpansion of paperboards. *Nordic Pulp & Paper Research Journal*, 12, 103–110.
4. Padanyi, Z. V. (1991). Mechano-sorptive effects and accelerated creep in paper. In *Proceedings of the International Paper Physics Conference* (Vol. 2, pp. 397–411). Atlanta: TAPPI Press.
5. Habeger, C. C., & Coffin, D. W. (2000). The role of stress concentrations in accelerated creep and sorption-induced physical aging. *Journal of Pulp and Paper Science*, 26, 145–157.
6. Chandoul, B. (2013). Étude des transferts massiques et thermiques dans les milieux poreux déformables non saturés: Application à la fabrication et au stockage de papier (Ph.D. thesis). Université de Gabès, ENIG.
7. Amir, H., Le Palec, G., & Daguene, M. (1987). Séchage superficiel d'un matériau poreux humide par convection forcée d'air chaud: Couplage entre les équations de transfert dans le matériau et celles de la couche limite. *International Journal of Heat and Mass Transfer*, 30(6), 1149–1158.
8. Mhimid, A., Ben Nasrallah, S., & Fohr, J. P. (2000). Heat and mass transfer during drying of granular products: Simulation with convective and conductive boundary conditions. *International Journal of Heat and Mass Transfer*, 43(15), 2779–2791.

Copyright: ©2026 Belgacem CHANDOUL, et al. This is an open-access article distributed under the terms of the Creative Commons Attribution License, which permits unrestricted use, distribution, and reproduction in any medium, provided the original author and source are credited.